

Waterproof and Tailorable Elastic Rechargeable Yarn Zinc Ion Batteries by a Cross-Linked Polyacrylamide Electrolyte

Hongfei Li,[†] Zhuoxin Liu,[†] Guojin Liang,[†] Yang Huang,[‡] Yan Huang,[§] Minshen Zhu,[†] Zengxia Pei,[†] Qi Xue,[†] Zijie Tang,[†] Yukun Wang,[†] Baohua Li,^{||} and Chunyi Zhi^{*,†,‡,§}

[†]Department of Materials Science and Engineering, City University of Hong Kong, 83 Tat Chee Avenue, Kowloon Tong, Hong Kong SAR, China

[‡]College of Materials Science and Engineering, Shenzhen University, Shenzhen 518000, China

[§]State Key Laboratory of Advanced Welding and Joining, Harbin Institute of Technology, Shenzhen 518055, China

^{||}Engineering Laboratory for the Next Generation Power and Energy Storage Batteries, Graduate School at Shenzhen, Tsinghua University, Shenzhen 518055, China

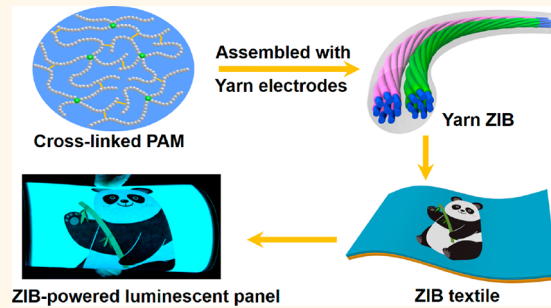
^{*}Shenzhen Research Institute, City University of Hong Kong, Shenzhen 518000, China

Supporting Information

ABSTRACT: Emerging research toward next-generation flexible and wearable electronics has stimulated the efforts to build highly wearable, durable, and deformable energy devices with excellent electrochemical performances. Here, we develop a high-performance, waterproof, tailorable, and stretchable yarn zinc ion battery (ZIB) using double-helix yarn electrodes and a cross-linked polyacrylamide (PAM) electrolyte. Due to the high ionic conductivity of the PAM electrolyte and helix structured electrodes, the yarn ZIB delivers a high specific capacity and volumetric energy density (302.1 mAh g^{-1} and 53.8 mWh cm^{-3} , respectively) as well as excellent cycling stability (98.5% capacity retention after 500 cycles).

More importantly, the quasi-solid-state yarn ZIB also demonstrates superior knittability, good stretchability (up to 300% strain), and superior waterproof capability (high capacity retention of 96.5% after 12 h underwater operation). In addition, the long yarn ZIB can be tailored into short ones, and each part still functions well. Owing to its weavable and tailorable nature, a 1.1 m long yarn ZIB was cut into eight parts and woven into a textile that was used to power a long flexible belt embedded with 100 LEDs and a 100 cm^2 flexible electroluminescent panel.

KEYWORDS: rechargeable zinc ion batteries, yarn battery, polyacrylamide, waterproof, stretchable



Flexible or wearable electronics are leading the trend of next-generation consumer electronic products, and they are finding more applications in sportswear, pressure sensors, military uniforms, and implantable medical devices.^{1–3} One of the key challenges identified in this field is how to fabricate highly deformable, durable, and wearable energy storage devices with excellent electrochemical performances and shape versatility.^{4–6} One-dimensional (1D) fiber or yarn-based energy devices may offer ideal solutions to these demands, owing to their light weight, tiny volume, and structural varieties. More importantly, 1D energy storage devices can be easily integrated with commercial textiles, which enable them to be more suitable than thin film devices for smart or wearable textile applications.^{7–12} In this context, great efforts have been made to develop different 1D linear power sources such as lithium ion batteries,^{13,14} lithium–sulfur

batteries,¹⁵ primary batteries,¹⁶ and supercapacitors.^{17–19} From the view of practical use, energy storage devices should be able to deliver high energy capacity while maintaining their electrochemical functions under different conditions, such as being bent, stretched, cut, or even washed in water. However, the current research in yarn batteries or power-type supercapacitors still falls greatly behind these requirements.

The Zn–MnO₂ battery has been considered to be one of the most popular primary cells over the past 100 years due to its low price, eco-friendliness, high specific capacity, and facile fabrication.²⁰ These attractive features, coupled with the increasing demand for high-performance flexible power sources,

Received: December 20, 2017

Accepted: March 6, 2018

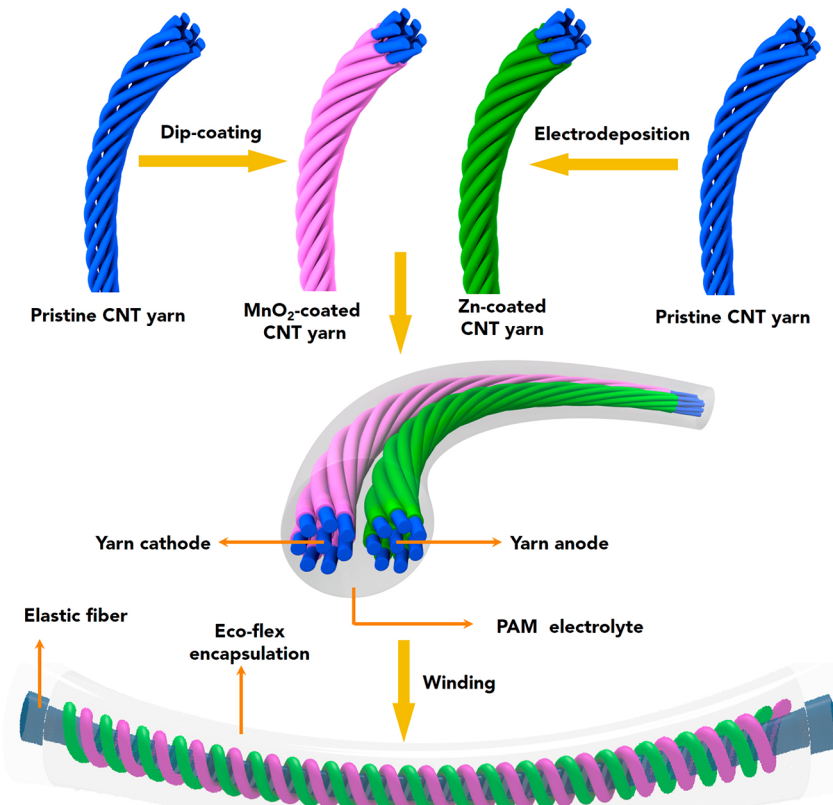


Figure 1. Schematic diagram of fabrication and encapsulation of the yarn ZIB.

have stimulated extensive research interests in developing flexible batteries based on the Zn–MnO₂ system. Yu *et al.* introduced a fiber-type primary Zn–MnO₂ using carbon fibers as a current collector.²¹ Gaikwad *et al.* and Wang *et al.* demonstrated a flexible alkaline battery based on polymer gel electrolytes, exhibiting superior discharge performance and good flexibility.^{22,23} However, these available flexible Zn–MnO₂ batteries are not rechargeable and suffer from sharp capacity attenuation. Recently, a rechargeable zinc ion battery (ZIB) was proposed, which successfully evolves the primary Zn–MnO₂ batteries into highly reversible energy storage systems.^{24–28} Nevertheless, 1D rechargeable yarn ZIBs with good wearability, high energy density, and excellent cycling performance remain a challenge.

A key component of the ZIB for the stretchable and wearable design is the solid-state or gel electrolyte. However, the widely used poly(vinyl alcohol) (PVA)-based electrolytes suffer from low elasticity, low ionic conductivity, and poor mechanical strength. By contrast, hydrogels, as hydrophilic polymer networks swollen with a large amount of water, can dissolve different kinds of ions, thus making them promising good ionic conductors.²⁹ In order to achieve a well-designed polymer–metal salt electrolyte, the selection of polymer host is of great importance.³⁰

Herein, we report the paradigm of a quasi-solid-state washable and tailorabile elastic yarn ZIB constructed by double-helix yarn electrodes and a polyacrylamide (PAM)-based polymer electrolyte. To achieve stable electrochemical performance under repetitive deformation conditions, we developed the PAM as the polyelectrolyte matrix host for the neutral solution of zinc sulfate and manganese sulfate. Due to the good compatibility between metal salts and PAM, the

developed polymer electrolyte possesses a high ionic conductivity and exceptional strength, which greatly enhance the rechargeability of the fabricated ZIBs. Double-helix carbon nanotube (CNT) yarns were used as substrates for the MnO₂ cathode and zinc anode, which effectively enhance the strength and robustness of the electrodes under different deformation conditions and significantly improve electrolyte wetting of the electrode surface. The fabricated quasi-solid-state yarn ZIB delivers a high specific capacity and volumetric energy density (302.1 mAh g⁻¹ and 53.8 mWh cm⁻³, respectively) as well as excellent cycling stability (98.5% capacity retention after 500 cycles at a high current of 2 A g⁻¹). Moreover, the quasi-solid-state yarn ZIB also demonstrates superior flexibility and stretchability (up to 300% strain), in conjunction with a high capacity retention of 96.5% after 12 h continuous underwater operation (in deionized water). In addition, a 1.1 m long yarn ZIB was tailored and woven into a battery textile that could power a long light-emitting diode (LED) belt and a 100 cm² electroluminescent panel.

RESULTS AND DISCUSSION

A typical fabrication process of the quasi-solid-state yarn ZIB is schematically illustrated in Figure 1. In particular, as the yarn battery must be eventually integrated into the modern textile industry for practical applications, here, we demonstrate a protocol which is ready to fabricate the yarn battery in large scale. The continuous CNT fiber, which is an assembly of aligned CNTs, possesses the multifunctional merits of CNTs. With intrinsic good mechanical and electrical properties, the helix-structured CNT fiber can maintain its structural integrity and good electrical conductivity after being bent, twisted, or

knotted several times, which makes it a desirable substrate for application in 1D wire-shaped batteries and supercapacitors.

As shown in Figure S1, roll-dip-coating and roll-electrodeposition processes were developed, which can produce the MnO₂ yarn cathode and zinc yarn anode continuously in a very facile way based on the CNT fibers. After being cleaned with deionized (DI) water and ethanol, eight CNT aligned fibers were twisted into a CNT yarn. Then the yarn was passed through a vessel filled with predispersed MnO₂ paste and fixed to a motor. As the motor steadily rotated at a slow rate of 0.1 cm s⁻¹, the MnO₂ paste was uniformly coated on the surface of helix-structured CNT yarn. The as-prepared MnO₂ yarn cathode was dried at room temperature in a vacuum for 6 h before use. For the fabrication of zinc anode, three stainless steel rods and zinc foils in the vessel were connected to the electrochemical station. Then a CNT yarn was guided through the rods in the vessel and fixed to the motor. As the motor steadily rotated, zinc was homogeneously deposited on the surface of CNT fibers. Then the yarn was washed by DI water several times and dried at room temperature in a vacuum for 6 h to finally obtain the zinc yarn anode. Subsequently, the MnO₂ yarn cathode and zinc yarn anode were further wound onto an elastic fiber in parallel, followed by coating PAM electrolyte on and between the two electrodes. Finally, the entire device was encapsulated with Eco-flex silicone and water repellent to render the yarn battery waterproof and stretchable (Figure 1).

The X-ray diffraction (XRD) pattern shows the crystalline phase of the MnO₂/CNT composite (Figure S2), in which diffraction peaks can be well-indexed to the characteristic peaks of α -MnO₂ (JCPDS: 44-0141). The scanning electron microscopy (SEM) images of the pristine CNT yarn used in this work are presented in Figure 2a,b. The CNT fiber has an average diameter of around 30 μm and a fairly compact structure, in which the CNTs are highly aligned (Figures 2b and S3a). Figure 2c,d shows the morphology of the yarn zinc anode at different magnifications. Rock-like zinc deposits in discrete assemblies are uniformly coated on the surface of CNT yarn. Layer-by-layer growth of zinc on individual deposits can be observed in the image (Figure S3b,c). The SEM image of the yarn MnO₂ cathode (Figure 2e,f) reveals that MnO₂ paste was homogeneously coated on the surface of CNT fibers.

Transmission electron microscopy (TEM) image in Figure 2g shows that MnO₂ nanorods are approximately 30 nm wide with lengths ranging from 100 to 300 nm. Acid-treated CNTs with external diameters of 10–30 nm are uniformly dispersed among MnO₂ nanorods. The high-resolution TEM (HRTEM) image further exhibits a lattice distance of 0.685 nm for the (110) plane of the one-dimensional α -MnO₂ nanorods (Figures 2f and S3d), revealing that as-prepared MnO₂ nanorods are highly crystalline.

For the PAM-based electrolyte, the polyacrylamide chains could form a network by covalent cross-links and hydrogen bonds (Figure 3a). In a typical fabrication process, acrylamide (AM, main monomer) powders were dissolved in DI water, followed by addition of potassium persulfate as an initiator and *N,N'*-methylenebis(acrylamide) as the cross-linker for polyacrylamide. After the solution was degassed in a vacuum chamber, the mixed solution was kept at 50 °C for 4 h and a cross-linked PAM hydrogel was obtained through a free-radical polymerization approach. Finally, the cross-linked PAM hydrogel was soaked in a mixed solution of 2 mol L⁻¹ ZnSO₄ and 0.1 mol L⁻¹ MnSO₄ to absorb significant amounts of water and ions to ensure good ionic conductivity. For the ZIB, the

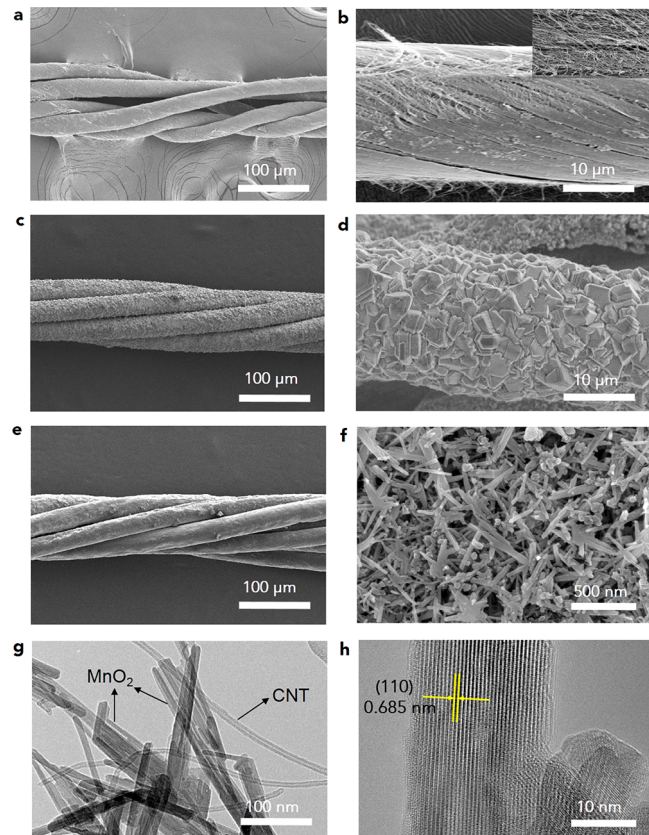


Figure 2. Microscope images of the yarn electrodes and MnO₂ nanorods. (a,b) SEM images of the pristine CNT fibers, (c,d) SEM images of the CNT@Zn yarn, (e,f) SEM images of the CNT@MnO₂ yarn, (g) TEM image, and (h) HRTEM image of the MnO₂ nanorods.

MnO₂ electrode usually suffers from a significant capacity fading due to the dissolution of Mn²⁺ ions through the disproportionation of Mn³⁺ during the charge/discharge processes.²⁵ The preadded MnSO₄ changes the dissolution equilibrium of Mn²⁺ ions and suppresses the dissolution of Mn²⁺ from MnO₂ into electrolyte, which is expected to effectively stabilize the MnO₂ electrode and enhance the cycling stability of the ZIB.

The as-prepared PAM electrolyte showed good tensile strength (273 kPa) and high stretchability to 3000% strain (Figures 3b and S4). The SEM image of freeze-dried PAM shows a highly porous network structure of the polymer matrix (Figure 3c), which is beneficial for the water trapping and free movement of zinc ions, endowing a good ionic conductivity. The ionic conductivity of the PAM hydrogel electrolyte containing 2 mol L⁻¹ ZnSO₄ and 0.1 mol L⁻¹ MnSO₄ obtained from the AC impedance spectra (Figure 3d) was calculated to be 17.3×10^{-3} S cm⁻¹ at room temperature. When subjected to a strain of 300%, the PAM-based electrolyte still shows a high ionic conductivity of 16.5×10^{-3} S cm⁻¹, demonstrating a stable and fast ionic transportation property under stretched conditions (Figure S5). Such a good ionic conductivity can be attributed to the presence of a highly porous network structure in the polymer matrix for zinc ions to move freely as well as a large number of hydrophilic groups such as amide groups ($-\text{CONH}_2$).

A Fourier transform infrared spectrum was used to elucidate the polymerization mechanism of the PAM solid electrolyte.

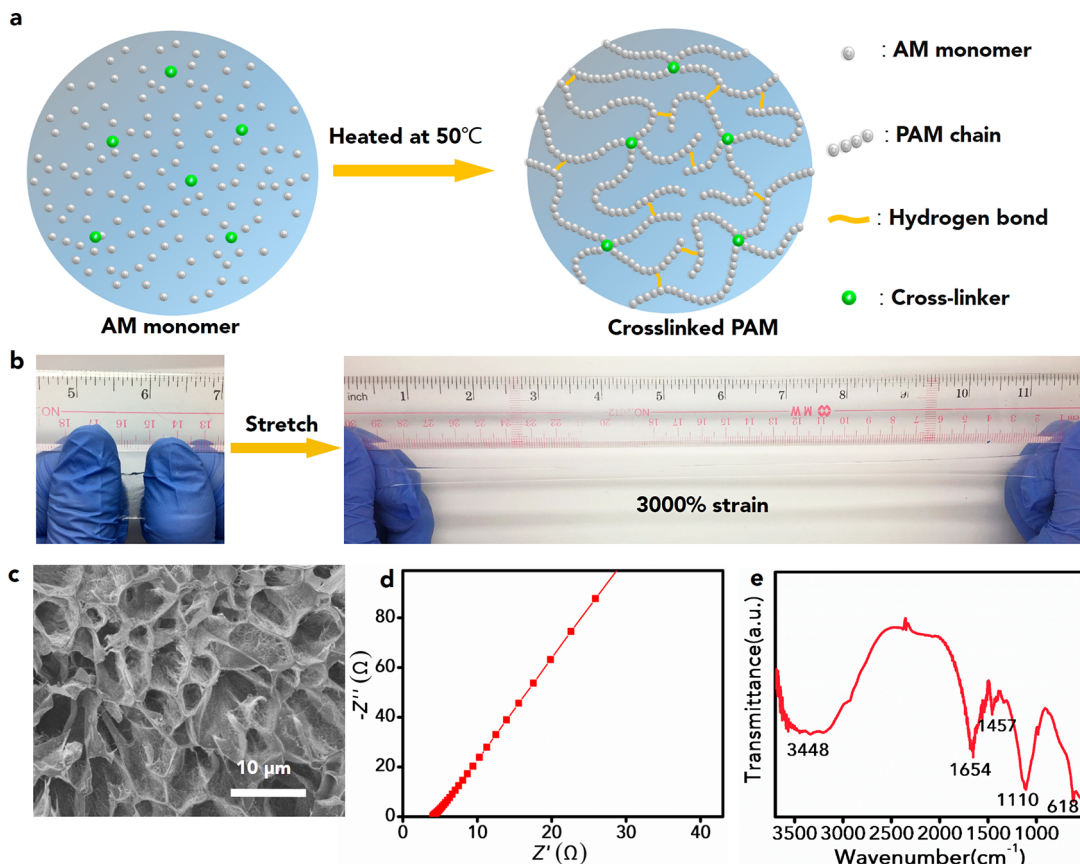


Figure 3. Schematic diagram and characterization of the cross-linked PAM based electrolyte. (a) Schematic diagram for the fabrication of the cross-linked PAM-based electrolyte. (b) Relaxed (left) and elongated (right) state of the cross-linked PAM, showing good stretchability (3000% strain). (c) SEM image of the free-standing PAM. (d) AC impedance spectra of the PAM in the frequency ranging from 10 kHz to 0.01 Hz. (e) Fourier transform infrared spectra of the PAM.

The spectrum of the pristine PAM (shown in Figure 3e) shows several absorption bands at 3448 cm^{-1} (N–H stretching vibration), 1654 cm^{-1} (amide I, C=O stretching vibration), and 1541 cm^{-1} (amide II, N–H bending vibration), which are typical absorption bands of PAM.^{31–34} Other bands at 1457 , 1110 , and 618 cm^{-1} are attributed to CH_2 scissoring, C–O stretching vibration, and N–H wagging vibration, respectively.³⁵

The electrochemical properties of the quasi-solid-state yarn ZIB under normal and various deformation conditions were evaluated by cyclic voltammetry (CV) measurements and galvanostatic charge/discharge tests (Figure 4). The CV curve was obtained at a sweep rate of 2 mV s^{-1} within the potential range of 1.0 – 2.0 V vs Zn/Zn^{2+} (Figure 4a). Two distinct peaks were observed at around 1.75 and 1.3 V from this curve, which should be attributed to the extraction/insertion of Zn^{2+} ions into/from the tunnel of MnO_2 crystals, respectively. The first and second charge/discharge curves of the quasi-solid-state yarn ZIB at a current of 60 mA g^{-1} are shown in Figure 4b. The fabricated yarn ZIB showed an open-circuit voltage of approximately 1.48 V . The yarn ZIB delivers reversible capacities of 283.6 and 302.1 mAh g^{-1} (based on MnO_2) at 60 mA g^{-1} in the initial two cycles, which are higher than the reported values.^{24,26–28} Moreover, the highest energy density of this yarn-shaped ZIB reached 53.8 mWh cm^{-3} , which is around 7 times larger than that of the Ni–Zn battery (7.76 mWh cm^{-3})³⁶ and 3 times that of the commercial thin film lithium ion battery (10 mWh cm^{-3}).³⁷ We also compared our device

with other energy storage devices, such as supercapacitors and yarn-based lithium ion batteries. Our developed yarn ZIB shows an advantageous energy density and simultaneously good stretchability and waterproof property (Table S1),^{38–42} which render it as a promising energy storage device for future flexible and wearable applications.

It is interesting that the rechargeable quasi-solid-state yarn ZIB shows rather different charge/discharge curves for the initial two cycles, and an obvious overpotential of about 300 mV was observed, which was quite similar to those of aqueous Zn/MnO_2 batteries reported previously.²⁵ It is believed that the morphology transformation and the changes of volume and surface energy of the nanostructured MnO_2 material during the charge and discharge process may contribute to this phenomenon.²⁵

Furthermore, the cycling test of the quasi-solid-state yarn ZIB was also carried out to evaluate its long-term cycling stability (Figure 4c). It exhibited a high capacity retention of 98.5% even after 500 cycles at a current density of 2 A g^{-1} (the initial specific capacity is 102.6 mAh g^{-1} at 2 A g^{-1}). This long-term cycling performance is mainly attributed to three determining factors: (1) The high water holding capacity and highly porous network of PAM can effectively trap a large amount of water in the matrix and hinder the water volatilization, which results in a high ionic conductivity and fast reaction kinetics throughout the long-term charge/discharge test. (2) The superior reactivity and interfacial stability between PAM-based electrolyte and electrodes

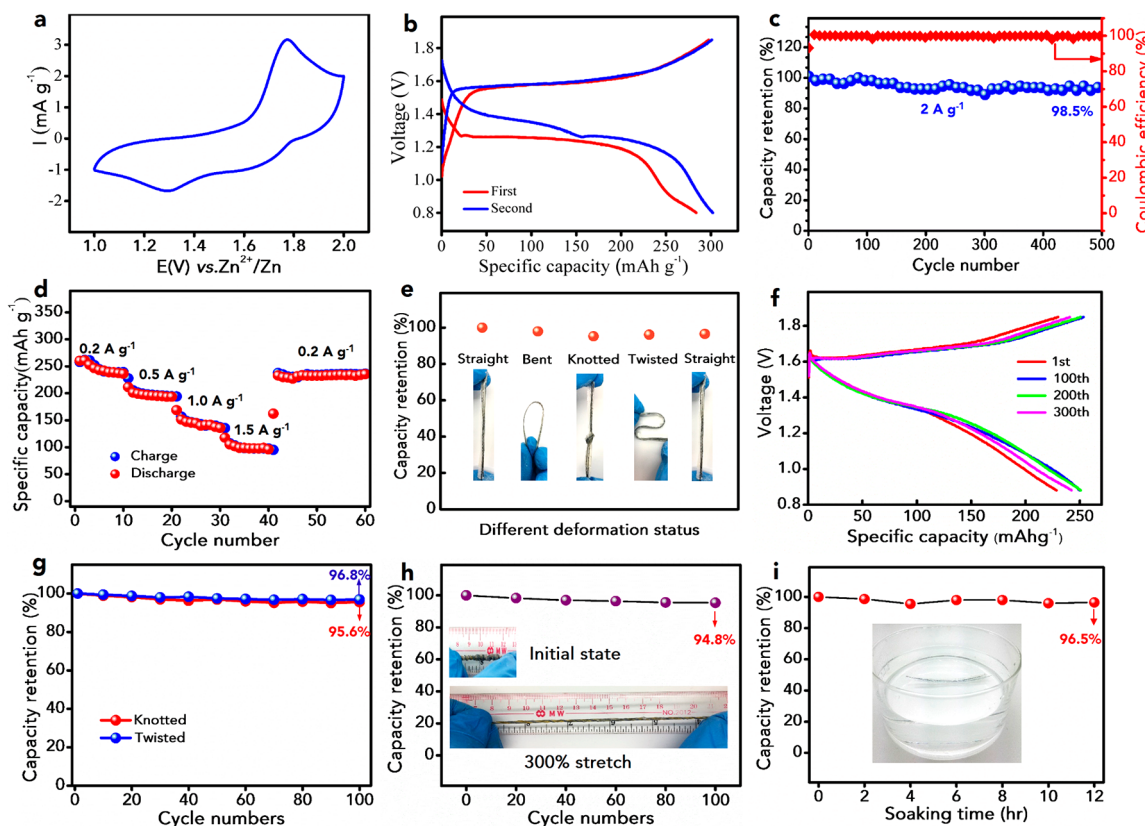


Figure 4. Electrochemical performance of the rechargeable yarn ZIB. (a) CV curve at a scan rate of 2 mVs^{-1} . (b) Initial two discharge/charge curves at a current density of 60 mA g^{-1} . (c) Long-term cycling performance and Coulombic efficiency at 2 A g^{-1} . (d) Rate capabilities at various current densities. (e) Capacity retention of the yarn ZIB under various deformation status. (f) Discharge curves of the yarn ZIB after different bending cycles. (g) Capacity retention of the yarn ZIB for 100 cycles under knotted and twisted conditions. (h) Dependence of capacity retention on cycle numbers with a strain of 300%. (i) Capacity retention test of the yarn ZIB for 12 h continuous underwater immersion in DI water at 24°C , showing superior waterproof ability. For (e–i), tests were performed at a current density of 0.3 A g^{-1} .

significantly lower the interfacial resistance during long-term charge/discharge cycles, which are of great importance for the cycling stability of quasi-solid-state yarn ZIB (Figure S6). (3) The well-dispersed CNTs in the MnO_2/CNT composite effectively enhance the electron transfer efficiency of the MnO_2 yarn cathode, which further improves the cycling stability of the quasi-solid-state ZIB.

The rate performance of the yarn batteries was also measured at various current densities ranging between 0.2 and 1.5 A g^{-1} by cycling it 10 times at each rate, and the results are presented in Figure 4d. The yarn battery exhibits high discharge capacities of 260.4 , 211.5 , 168.7 , and 117.7 mAh g^{-1} at current densities of 0.2 , 0.5 , 1 , and 1.5 A g^{-1} , respectively. After being cycled at a current density as high as 1.5 A g^{-1} , an average discharge capacity of 235.8 mAh g^{-1} is still recovered at a current density of 0.2 A g^{-1} , which is equivalent to 96.5% of the initial average capacity (244.3 mAh g^{-1}). The high rate performance could be ascribed to the stabilization of the electrodes and the high ionic conductivity of the PAM-based electrolyte.

To evaluate the durability and stability under different deformation conditions, yarn ZIBs were further subjected to a continuous deformation test. It can be seen that the capacity retention of the yarn battery remains above 95% under various deformation conditions in the order of being bent, knotted, and twisted (Figure 4e). After these nonplanar deformation tests, the yarn battery was recovered back to its original shape with over 95.8% of initial capacity remaining (Figure S7). The bending stability of the solid-state ZIB was tested by bending a

solid-state yarn ZIB at a bending angle of 90° for 300 times using a specially designed stepper motor (Figure 4f). It can be seen that there is only a slight change in these discharge curves, and over 93.6% capacity was retained after 300 continuous bending cycles. Cycling test results under knotted and twisted conditions are shown in Figure 4g. It retains over 95.6 and 96.8% of the initial discharge capacity after charging and discharging for 100 times under knotting and twisting conditions, respectively. The yarn ZIB maintained a high capacity retention of 94.8% after cycling 100 times when a strain of 300% was applied, which is close to the value of 97.2% under normal conditions (Figure 4h and Figure S8). The high robustness and electrochemical stability of yarn ZIBs under various deformation conditions are beneficial for the practical applications in flexible and wearable devices.

When integrated with electronics or textiles, the yarn battery may occasionally get wet by the rain or splashes of water during daily use. Therefore, the waterproof capability of an energy storage unit is also a key factor for future wearable applications.⁴³ Unlike traditional packaging, the yarn battery encapsulated with Eco-flex silicone can achieve a superior waterproof performance while maintaining a high stretchability and flexibility. It can be seen that the yarn ZIB has a capacity retention of 96.5% after being fully immersed in water for 12 h, demonstrating good waterproof capability and high durability (Figures 4i and S9). The SEM images of the MnO_2 cathode and Zn anode after charge/discharge tests under different deformation conditions were also measured and are shown in

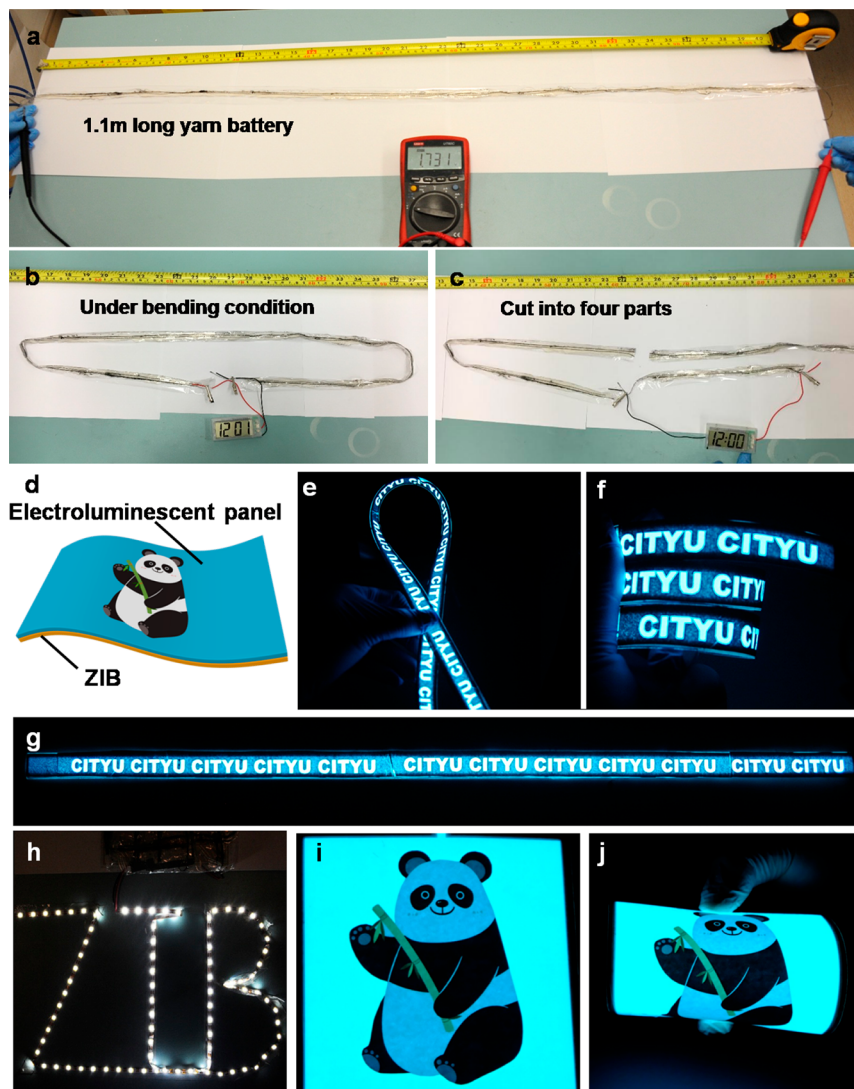


Figure 5. Tailoring test and demonstration of solid-state yarn ZIBs. (a) Optical image of the as-prepared 1.1 m long yarn ZIB. (b) Long yarn ZIB under bending condition. (c) Long yarn battery was cut into four parts, and each part can power the digital watch. (d) Schematic diagram of a flexible battery display unit system. (e–g) Eight yarn batteries were connected in series to power a 1 m long electroluminescent panel (size 1.0×100 cm) under different bending conditions. (h) Eight segmented yarn batteries were connected in series to power a long LED belt consisting of 100 lamp beads. (i,j) Eight segmented yarn batteries were connected in series to power a 100 cm^2 electroluminescent panel (size 10.0×10.0 cm) under different bending conditions.

Figure S10. The integrity of the yarn Zn anode and MnO_2 cathode was well maintained, and no obvious crack was observed due to the good protection of the elastic PAM-based electrolyte.

One intriguing point of the rechargeable yarn-based ZIB is its good tailorability and weavability. Different from conventional coin, column, or square-shaped batteries, the yarn ZIB can be cut to any desired length to meet the requirement of high-level integration, catering to versatile applications ranging from cloth to smart glasses, smart watches, and flexible displays. As shown in Figure 5a, a 1.1 m long yarn ZIB was fabricated by the facile roll-dipping and roll-electrodeposition processes as mentioned previously. When it was cut into two parts, each of them can power a digital watch (Figure 5b). Even when the yarn battery was further cut into eight parts, each segmented battery could drive the electronic watch, showing high reliability (Figure 5c). Moreover, when these eight segmented yarn batteries were woven into a battery textile, they could power a 1 m long LED

belt consisting of 100 lamp beads or a 100 cm^2 flexible electroluminescent panel via a small booster (Figures 5d–j and S11). These features indicate that the solid-state ZIB can serve as a powerful and reliable energy storage device for more practical applications in other fields, including sensors, implantable medical devices, robotics, and so on.

CONCLUSIONS

In summary, we have successfully constructed a high-performance waterproof and stretchable yarn zinc ion battery by double-helix yarn electrodes and a cross-linked PAM-based polymer electrolyte. The PAM electrolyte not only acts an effective separator but also serves as a good ionic conductor. This ZIB delivers a high specific capacity and volumetric energy density (302.1 mAh g^{-1} and 53.8 mWh cm^{-3} , respectively) as well as excellent cycling stability (98.5% capacity retention after 500 cycles). More importantly, the solid-state yarn ZIB also demonstrates good tailorability, knittability, and stretchability

(up to 300% strain) as well as superior waterproof capability (96.5% capacity retention after 12 h soaking). These properties, combined with high electrochemical performance, enable our yarn ZIBs to serve as promising and reliable energy storage devices for flexible and wearable applications.

EXPERIMENTAL SECTION

Preparation of Cross-Linked PAM Electrolyte. Two grams of acrylamide monomer powders was added into 20 g of DI water and stirred for 30 min at 25 °C to fully dissolve. Then, 10 mg of potassium persulfate (initiator) and 2 mg of *N,N'*-methylenebis(acrylamide) (cross-linker) were added into the above solution and stirred for 1 h at 25 °C. After the solution was degassed in a vacuum chamber, the mixed solution was poured into a stainless steel mold and kept at 50 °C for 4 h to obtain a cross-linked PAM hydrogel *via* a free-radical polymerization approach. Finally, the cross-linked PAM hydrogel was soaked in 400 mL of mixed solution of 2 mol L⁻¹ ZnSO₄ and 0.1 mol L⁻¹ MnSO₄ up to 72 h to achieve the equilibrated state.

Preparation of the MnO₂ Cathode. The MnO₂/CNT composite was synthesized by a modified co-precipitation and hydrothermal method. In a typical synthesis run, 0.1 g of multiwalled CNTs with a length of 5–10 μm (Shenzhen Nanotech Port Co., Ltd.) was purified by refluxing the as-received sample in nitric acid (AR grade, 68 wt %, Aladdin) for 6 h at 80 °C. The acid-treated CNT was washed with DI water several times and finally redispersed in 150 mL of DI water. Then, 2.94 g of Mn(CH₃COO)₂·4H₂O (AR grade, Aladdin) was added into the above solution under continuous stirring for 0.5 h. Subsequently, the above solution was added dropwise into an aqueous solution prepared by dissolving 1.27 g of KMnO₄ (AR grade, Aladdin) into 80 mL of DI water and stirring for 0.5 h. The mixed solution was then blended intensively by an ultrasonic mixer for 10 min and transferred to a Teflon-lined autoclave and heated at 120 °C for 12 h. After being cooled, the obtained dark brown precipitate was washed several times with DI water and dried at room temperature in a vacuum oven for 8 h to finally obtain the MnO₂/CNT composite. MnO₂ paste was prepared by blending the MnO₂/CNT composite, acetylene black, and polytetrafluoroethylene at a weight ratio of 7:2:1 with DI water as solvent.

A roll-dip-coating was developed to produce the MnO₂ yarn cathode continuously in a facile way. After being cleaned with DI water and ethanol, eight CNT aligned fibers (Suzhou Hengqiu Technology Co., Ltd.) were twisted into a CNT yarn. Then the yarn was passed through a vessel filled with predispersed MnO₂ paste and fixed to a motor. As the motor steadily rotated at a slow rate of 0.1 cm s⁻¹, the MnO₂ paste was uniformly coated on the surface of the CNT yarn. Then the yarn was dried at room temperature in vacuum for 6 h to finally obtain the MnO₂ cathode. The effective mass loading of MnO₂ is 2.5–5.0 mg cm⁻².

Preparation of the Zn Anode. A flexible Zn electrode was prepared by a facile roll-electrodeposition approach on the CNT fibers. A typical two-electrode setup was used for Zn electroplating, in which the CNT fiber substrate was used as a working electrode, whereas a zinc plate (purity >99.99%, Sigma) was used as both counter and reference electrode. Aqueous solution containing 1 mol L⁻¹ ZnSO₄ (AR grade, Sigma) and 1 mol L⁻¹ KCl (AR grade, Sigma) was used as electrolyte. For the fabrication of the zinc anode, three stainless steel rods and zinc foils in the vessel were connected to the electrochemical station. Then a CNT yarn was guided through the rods in the vessel and fixed to the motor. As the motor steadily rotated, the zinc was uniformly deposited on the surface of CNT fibers. Electroplating was performed at −0.8 V *vs* Zn foil for 1000–2000 s using an electrochemical workstation (CHI 760D). Then the yarn was washed with DI water several times and dried at room temperature in a vacuum for 6 h to finally obtain the Zn yarn anode. The effective mass loading of zinc is 3.5–7.0 mg cm⁻².

Characterization Methods. Structural and phase characterizations of the as-prepared solid electrolyte films and electrodes were done by XRD using a Bruker D2 Phaser diffractometer with Cu K α irradiation ($\lambda = 1.54 \text{ \AA}$). The morphology of these samples was

measured by a scanning electron microscope (ESEM, FEI/Philips XL30). The high-resolution morphology and microstructure of the samples were characterized by a JEOL-2001F field-emission TEM.

Electrochemical Measurements. Cyclic voltammetry curves and electrochemical impedance spectroscopy (100 kHz to 0.1 Hz) were conducted by an electrochemical workstation (CHI 760D). The yarn ZIB was assembled by winding the MnO₂ yarn cathode and zinc yarn anode onto an elastic fiber in parallel, followed by coating PAM electrolyte on and between the two electrodes. Then the yarn ZIB was encapsulated with Eco-flex silicone and cured at room temperature for 6 h. Electrochemical performance of the prepared ZIB were examined based on galvanostatic testing in the voltage range of 0.8–1.85 V using a Land 2001A battery testing system at 24 °C. The volumetric energy density (*E*) of the full battery was calculated by

$$E = \int_0^t IV_{(t)} dt / V \quad (1)$$

where *I* is the discharge current, *V_(t)* is the discharge voltage at time *t*, *dt* is time differential, and *V* is the total volume of the whole solid-state device, which is calculated by multiplying the cross-sectional area and the length of the yarn ZIB (the total volume of the tested device ranges from 0.0157 to 0.0393 cm³). The ionic conductivity of polymer electrolyte can be calculated by ohmic resistance, which can be obtained from AC impedance spectra. The equation of ionic conductivity *c* was calculated by

$$\sigma = \frac{l}{RA} \quad (2)$$

where σ is ionic conductivity of polymer electrolyte, and *l*, *R*, and *A* represent the thickness, the bulk resistance, and the test area of polymer electrolyte, respectively.

ASSOCIATED CONTENT

S Supporting Information

The Supporting Information is available free of charge on the ACS Publications website at DOI: [10.1021/acsnano.7b09003](https://doi.org/10.1021/acsnano.7b09003).

Figures S1–S11 and Table S1 (PDF)

AUTHOR INFORMATION

Corresponding Author

*E-mail: cy.zhi@cityu.edu.hk.

ORCID

Yang Huang: [0000-0001-5060-3414](https://orcid.org/0000-0001-5060-3414)

Chunyi Zhi: [0000-0001-6766-5953](https://orcid.org/0000-0001-6766-5953)

Author Contributions

C.Z. and H.L. proposed and designed the research. H.L. and Z.L. carried out the fabrication of PAM, cathode, anode, as well as the yarn ZIB. G.L., Y.H. (Yang Huang), Y.H. (Yan Huang), M.Z., and H.L. performed the characterization and electrochemical measurements. Z.P. and Q.X. carried out the deformation test. Z.T. and Y.W. performed the demonstration of ZIBs. H.L., B.L., and C.Z. analyzed the experimental results and co-wrote the manuscript. All authors discussed the experimental results and commented on the manuscript.

Notes

The authors declare no competing financial interest.

ACKNOWLEDGMENTS

This work was sponsored by the NSFC/RGC Joint Research Scheme under Project N_CityU123/15 and City University of Hong Kong (PJ7004645). The work was also partially sponsored by the project 2017JY0088 supported by Science & Technology Department of Sichuan Province and was

partially supported by the Chengdu Research Institute, City University of Hong Kong.

REFERENCES

- (1) Kim, D. H.; Kim, Y. S.; Amsden, J.; Panilaitis, B.; Kaplan, D. L.; Omenetto, F. G.; Zakin, M. R.; Rogers, J. A. Silicon Electronics on Silk as a Path to Bioresorbable, Implantable Devices. *Appl. Phys. Lett.* **2009**, *95*, 133701.
- (2) Fu, K. K.; Cheng, J.; Li, T.; Hu, L. Flexible Batteries: From Mechanics to Devices. *ACS Energy Lett.* **2016**, *1*, 1065–1079.
- (3) Gulzar, U.; Goriparti, S.; Miele, E.; Li, T.; Maidecchi, G.; Toma, A.; De Angelis, F.; Capiglia, C.; Zaccaria, R. P. Next-Generation Textiles: From Embedded Supercapacitors to Lithium Ion Batteries. *J. Mater. Chem. A* **2016**, *4*, 16771.
- (4) Lu, X.; Yu, M.; Wang, G.; Tong, Y.; Li, Y. Flexible Solid-State Supercapacitors: Design, Fabrication and Applications. *Energy Environ. Sci.* **2014**, *7*, 2160–2181.
- (5) Yu, D.; Zhai, S.; Jiang, W.; Goh, K.; Wei, L.; Chen, X.; Jiang, R.; Chen, Y. Transforming Pristine Carbon Fiber Tows into High Performance Solid-State Fiber Supercapacitors. *Adv. Mater.* **2015**, *27*, 4895–4901.
- (6) Zhou, G.; Li, F.; Cheng, H. M. Progress in Flexible Lithium Batteries and Future Prospects. *Energy Environ. Sci.* **2014**, *7*, 1307–1338.
- (7) Huang, Y.; Zhu, M.; Huang, Y.; Li, H.; Pei, Z.; Xue, Q.; Liao, Z.; Wang, Z.; Zhi, C. A Modularization Approach for Linear-Shaped Functional Supercapacitors. *J. Mater. Chem. A* **2016**, *4*, 4580–4586.
- (8) Lee, Y. H.; Kim, J. S.; Noh, J.; Lee, I.; Kim, H. J.; Choi, S.; Seo, J.; Jeon, S.; Kim, T. S.; Lee, J. Y.; Choi, J. W. Wearable Textile Battery Rechargeable by Solar Energy. *Nano Lett.* **2013**, *13*, 5753–5761.
- (9) Wang, X.; Jiang, K.; Shen, G. Flexible Fiber Energy Storage and Integrated Devices: Recent Progress and Perspectives. *Mater. Today* **2015**, *18*, 265–272.
- (10) Wang, Y.; Chen, C.; Xie, H.; Gao, T.; Yao, Y.; Pastel, G.; Han, X.; Li, Y.; Zhao, J.; Fu, K.; Hu, L. 3D printed-All Fiber Li-ion Battery toward Wearable Energy Storage. *Adv. Funct. Mater.* **2017**, *27*, 1703140.
- (11) Huang, Y.; IP, W. S.; Lau, Y. Y.; Sun, J.; Zeng, J.; Yeung, N. S. S.; Ng, W. S.; Li, H.; Pei, Z.; Xue, Q.; Wang, Y.; Yu, J.; Hu, H.; Zhi, C. A Weavable, Conductive Yarn-Based NiCo//Zn Textile with High Energy Density and Rate Capability. *ACS Nano* **2017**, *11*, 8953–8961.
- (12) Zhang, Y.; Zhao, Y.; Cheng, X.; Weng, W.; Ren, J.; Fang, X.; Jiang, Y.; Chen, P.; Zhang, Z.; Wang, Y.; Peng, H. Realizing both High Energy and High Power Densities by Twisting Three Carbon-Nanotube-Based Hybrid Fibers. *Angew. Chem., Int. Ed.* **2015**, *54*, 11177–11182.
- (13) Kwon, Y. H.; Woo, S. W.; Jung, H. R.; Yu, H. K.; Kim, K.; Oh, B. H.; Ahn, S.; Lee, S. Y.; Song, S. W.; Cho, J.; Shin, H. C.; Kim, J. Y. Cable-Type Flexible Lithium Ion Battery Based on Hollow Multi-Helix Electrodes. *Adv. Mater.* **2012**, *24*, 5192–5197.
- (14) Hoshide, T.; Zheng, Y.; Hou, J.; Wang, Z.; Li, Q.; Zhao, Z.; Ma, R.; Sasaki, T.; Geng, F. A Flexible Lithium-Ion Fiber Battery by Regularly Stacking Two-Dimensional Titanium Oxide Nanosheets Hybridized with Reduced Graphene Oxide. *Nano Lett.* **2017**, *17*, 3543–3549.
- (15) Fang, X.; Weng, W.; Ren, J.; Peng, H. A Cable-Shaped Lithium Sulfur Battery. *Adv. Adv. Mater.* **2016**, *28*, 491–496.
- (16) Qu, H.; Semenikhin, O.; Skorobogatiy, M. Flexible Fiber Batteries for Applications in Smart Textiles. *Smart Mater. Struct.* **2015**, *24*, 025012.
- (17) Kou, L.; Huang, T.; Zheng, B.; Han, Y.; Zhao, X.; Gopalsamy, K.; Sun, H.; Gao, C. Coaxial Wet-Spun Yarn Supercapacitors for High-Energy Density and Safe Wearable Electronics. *Nat. Commun.* **2014**, *5*, 3754.
- (18) Choi, C.; Kim, K. M.; Kim, K. J.; Lepró, X.; Spinks, G. M.; Baughman, R. H.; Kim, S. J. Improvement of System Capacitance via Weavable Superelastic Biscrolled Yarn Supercapacitors. *Nat. Commun.* **2016**, *7*, 13811.
- (19) Yu, D.; Goh, K.; Wang, H.; Wei, L.; Jiang, W.; Zhang, Q.; Dai, L.; Chen, Y. Scalable Synthesis of Hierarchically Structured Carbon Nanotube-Graphene Fibres for Capacitive Energy Storage. *Nat. Nanotechnol.* **2014**, *9*, 555–562.
- (20) Shen, Y. W.; Kordesch, K. The Mechanism of Capacity Fade of Rechargeable Alkaline Manganese Dioxide Zinc Cells. *J. Power Sources* **2000**, *87*, 162–166.
- (21) Yu, X.; Fu, Y.; Cai, X.; Kafafy, H.; Wu, H.; Peng, M.; Hou, S.; Lv, Z.; Ye, S.; Zou, D. Flexible Fiber-Type Zinc-Carbon Battery Based on Carbon Fiber Electrodes. *Nano Energy* **2013**, *2*, 1242–1248.
- (22) Gaikwad, A. M.; Whiting, G. L.; Steingart, D. A.; Arias, A. C. Highly Flexible, Printed Alkaline Batteries Based on Mesh-Embedded Electrodes. *Adv. Mater.* **2011**, *23*, 3251–3255.
- (23) Wang, Z.; Wu, Z.; Bramnik, N.; Mitra, S. Fabrication of High-Performance Flexible Alkaline Batteries by Implementing Multiwalled Carbon Nanotubes and Copolymer Separator. *Adv. Mater.* **2014**, *26*, 970–976.
- (24) Xu, C.; Li, B.; Du, H.; Kang, F. Energetic Zinc Ion Chemistry: The Rechargeable Zinc Ion Battery. *Angew. Chem., Int. Ed.* **2012**, *51*, 933–935.
- (25) Pan, H.; Shao, Y.; Yan, P.; Cheng, Y.; Han, K. S.; Nie, Z.; Wang, C.; Yang, J.; Li, X.; Bhattacharya, P.; Mueller, K. T.; Liu, J. Reversible Aqueous Zinc/Manganese Oxide Energy Storage from Conversion Reactions. *Nat. Energy* **2016**, *1*, 16039.
- (26) Lee, B.; Yoon, C. S.; Lee, H. R.; Chung, K. Y.; Cho, B. W.; Oh, S. H. Electrochemically-Induced Reversible Transition from the Tunneled to Layered Polymorphs of Manganese Dioxide. *Sci. Rep.* **2015**, *4*, 6066–6074.
- (27) Alfaruqi, M. H.; Gim, J.; Kim, S.; Song, J.; Pham, D. T.; Jo, J.; Xiu, Z.; Mathew, V.; Kim, J. A Layered δ -MnO₂ Nanoflake Cathode with High Zinc-Storage Capacities for Eco-Friendly Battery Applications. *Electrochim. Commun.* **2015**, *60*, 121–125.
- (28) Alfaruqi, M. H.; Mathew, V.; Gim, J.; Kim, S.; Song, J.; Baboo, J. P.; Choi, S. H.; Kim, J. Electrochemically Induced Structural Transformation in a γ -MnO₂ Cathode of a High Capacity Zinc-Ion Battery System. *Chem. Mater.* **2015**, *27*, 3609–3620.
- (29) Huang, Y.; Zhong, M.; Shi, F.; Liu, X.; Tang, Z.; Wang, Y.; Huang, Y.; Hou, H.; Xie, X.; Zhi, C. An intrinsically stretchable and compressible supercapacitor containing a polyacrylamide hydrogel electrolyte. *Angew. Chem., Int. Ed.* **2017**, *56*, 9141–9145.
- (30) Choudhury, N. A.; Sampath, S.; Shukla, A. K. Hydrogel-Polymer Electrolytes for Electrochemical Capacitors: An Overview. *Energy Environ. Sci.* **2009**, *2*, 55–67.
- (31) Yang, F.; Li, G.; He, Y. G.; Ren, F. X.; Wang, G. X. Synthesis, Characterization, and Applied Properties of Carboxymethyl Cellulose and Polyacrylamide Graft Copolymer. *Carbohydr. Polym.* **2009**, *78*, 95–99.
- (32) Hu, X.; Feng, L.; Xie, A.; Wei, W.; Wang, S.; Zhang, J.; Dong, W. Synthesis and Characterization of a Novel Hydrogel: Salecan/Polyacrylamide Semi-IPN Hydrogel with a Desirable Pore Structure. *J. Mater. Chem. B* **2014**, *2*, 3646–3658.
- (33) Ghosh, P.; Chakrabarti, A.; Siddhanta, S. K. Studies on Stable Aqueous Polyaniline Prepared with the Use of Polyacrylamide as the Water Soluble Support Polymer. *Eur. Polym. J.* **1999**, *35*, 803–813.
- (34) Biswal, D. R.; Singh, R. P. Flocculation Studies Based on Water-Soluble Polymers of Grafted Carboxymethyl Cellulose and Polyacrylamide. *J. Appl. Polym. Sci.* **2006**, *102*, 1000–1007.
- (35) Biswal, D. R.; Singh, R. P. Characterisation of Carboxymethyl Cellulose and Polyacrylamide Graft Copolymer. *Carbohydr. Polym.* **2004**, *57*, 379–387.
- (36) Liu, J.; Guan, C.; Zhou, C.; Fan, Z.; Ke, Q.; Zhang, G.; Liu, C.; Wang, J. A Flexible Quasi-Solid-State Nickel-Zinc Battery with High Energy and Power Densities Based on 3D Electrode Design. *Adv. Mater.* **2016**, *28*, 8732–8739.
- (37) Pech, D.; Brunet, M.; Durou, H.; Huang, P.; Mochalin, V.; Gogotsi, Y.; Taberna, P. L.; Simon, P. Ultrahigh-Power Micrometre-Sized Supercapacitors Based on Onion-Like Carbon. *Nat. Nanotechnol.* **2010**, *5*, 651–654.

- (38) Chen, C.; Zhang, Y.; Li, Y.; Dai, J.; Song, J.; Yao, Y.; Gong, Y.; Kierzewski, I.; Xie, J.; Hu, L. All-wood, Low Tortuosity, Aqueous, Biodegradable Supercapacitors with Ultra-High Capacitance. *Energy Environ. Sci.* **2017**, *10*, 538–545.
- (39) Yuan, Z.; Peng, H. J.; Huang, J. Q.; Liu, X. Y.; Wang, D. W.; Cheng, X. B.; Zhang, Q. Hierarchical Free-Standing Carbon-Nanotube Paper Electrodes with Ultrahigh Sulfur-Loading for Lithium-Sulfur Batteries. *Adv. Funct. Mater.* **2014**, *24*, 6105–6112.
- (40) Hu, L.; Chen, W.; Xie, X.; Liu, N.; Yang, Y.; Wu, H.; Yao, Y.; Pasta, M.; Alshareef, H. N.; Cui, Y. Symmetrical MnO₂-Carbon Nanotube-Textile Nanostructures for Wearable Pseudocapacitors with High Mass Loading. *ACS Nano* **2011**, *5*, 8904–8913.
- (41) Zhou, C.; Zhang, Y.; Li, Y.; Liu, J. Construction of High-Capacitance 3D CoO@ Polypyrrole Nanowire Array Electrode for Aqueous Asymmetric Supercapacitor. *Nano Lett.* **2013**, *13*, 2078–2085.
- (42) Zhu, M.; Huang, Y.; Huang, Y.; Li, H.; Wang, Z.; Pei, Z.; Xue, Q.; Geng, H.; Zhi, C. A Highly Durable, Transferable, and Substrate-Versatile High-Performance All-Polymer Micro-Supercapacitor with Plug-and-Play Function. *Adv. Mater.* **2017**, *29*, 1605137.
- (43) Yang, Y.; Huang, Q.; Niu, L.; Wang, D.; Yan, C.; She, Y.; Zheng, Z. Waterproof, Ultrahigh Areal-Capacitance, Wearable Supercapacitor Fabrics. *Adv. Mater.* **2017**, *29*, 1606679.